Presumed PDF Modeling of Reactive
Oxy-Fuel Flow in a Model Combustor

■

S. A. Hashemi[1*], A. Fattahi[2], G. A. Sheikhzadeh[3]

■

[1] Department of Mechanical Engineering (Assistant Professor), University of Kashan, Kashan, I.R. Iran
Hashemi@kashanu.ac.ir

[2]Department of Mechanical Engineering (MSc student), University of Kashan, Kashan, I.R. Iran
abolfazl.fattahi@yahoo.com

[3]Department of Mechanical Engineering (Associate Professor), University of Kashan, Kashan, I.R. Iran
sheikhz@kashanu.ac.ir

■

Abstract

A non-premixed coaxial oxy-fuel turbulent flame was studied numerically with standard and realizable k-ε turbulence model and a comparison was made between them. The governing equations were solved by finite volume approach and were discretized using the second order upwind scheme. The presumed β-PDF model was applied to model turbulence-combustion interaction. The discrete ordinate radiation heat transfer method was also used. Comparison of numerical and experimental data showed that the realizable model has a better prediction of the axial velocity and NO concentration than that of the standard model.

Keywords: Oxy-fuel flame, Turbulence model, PDF model, Numerical simulation, NO_x pollutant.

✳ **Corresponding Author**

1. Introduction

Using oxygen instead of air has some advantages such as lower NO_x and higher temperature flames providing higher efficiency which is important for energy saving in combustion systems. In air-fuel systems, some of the energy of the fuel is consumed for increasing the temperature of nitrogen which exits from the exhaust in relatively high temperatures. Besides, for high temperature fuel-air systems, increasing the flame temperature causes higher NO_x formation rate (which strongly depends on temperature). Fossil fuels are employed in many industrial applications to produce thermal energy. Some parameters mainly affect the combustion of the fuel in a combustion system such as geometry of the combustor, mixing type of the fuel and oxidant, flow Reynolds number, inlet turbulence intensity, and inlet boundary condition. The interaction between turbulence and combustion is very important in the design of a combustion system. To design a combustion process considering turbulence effect, various simulations and parametric studies are necessary.

Numerical simulation techniques based on CFD (Computational fluid dynamics) analyses are suitable tools for in-depth comprehending of the systems. It can also be utilized to find the effective parameters and probable defects of the numerical model.

Employing an appropriate turbulence model is a main task in a flow with turbulent nature. The standard k-ε eddy viscosity model (Ske), which is a complete and simple model, is widely used in various turbulence computational fluid dynamics models such as in near-wall turbulent flows [l-4] and in rotating turbulent flows [5]. It is shown that Ske turbulence model can relatively predict the flow and temperature distributions for a reacting flow [6]. However, this model is not appropriate for flows with a high mean shear rate or a massive separation. Hence, for dominating these defects, the realizable turbulence model (Rke) was introduced with a new formulation for the turbulent viscosity.

Numerous experimental and numerical studies have been carried out on the turbulent combustion of non-premixed flames. Ellzey et al. [7] simulated an axisymmetric confined diffusion flame formed between a H_2-N_2 jet and compared their results with an analytical solution. They showed that if diffusion coefficients and densities are variable, small radial velocities are induced and the flame interface is somewhat deformed.

The PDF (probability density function) models with a fast chemistry assumption can be employed to consider the reaction–turbulence interactions. There are three functions of the PDF used in the modeling of turbulent reacting flows: the double δ function, the clipped Gaussian function, and the β function with two average methods: the Favre and the Reynolds methods [8]. Among them, β-PDF proposed and validated by Hannon et al. [9], shows comparatively better results for a turbulent reacting flow.

Hartick et al. [10] proposed a new approach for modeling turbulence-radiation interaction in a confined diffusion flame. They showed that considerable fluctuations of heat-release rate with constant mixture fraction happen at all positions. In addition, the coupling model that was made by means of a two-dimensional PDF of mixture fraction and heat-release rate has very little effect on the temperature-velocity and mixture fraction fields. Sautet et al. [11] measured the first and second order velocity moments and shear stresses for a 25kW, turbulent diffusion flame with natural gas-oxygen feed. They fitted the obtained radial velocity (V) by a Gaussian function. Aroussi et al. [12] studied the effect of one, two, and four burners on fluid velocity in a furnace experimentally and computationally. They used the second order differencing scheme with Ske turbulent model and showed that the flow characteristics were under-predicted by the solver for a single burner. Liakos et al. [13] investigated a two-dimensional model of a non-premixed natural gas flame under high strain. Three turbulence models were assessed and evaluated with respect to accurate prediction of the turbulence characteristics of the flame. They also analyzed the controlling mechanisms of the combustion process. Demoulin and Borghi [14] made an attempt to extend an approach used in PDF modeling of gaseous turbulent combustion to spray turbulent combustion by focusing on the new random fluctuations created by the spray. They tested their model with an experiment where one set of experimental conditions was close to the infinitely fast chemistry and another set of conditions demonstrated the effect of finite rate chemical kinetics. Repp et al. [15] compared two models for turbulence-chemistry interaction, including a Monte Carlo and a presumed β-PDF in a confined diffusion flame. They showed that both PDF models present a similar accuracy level of prediction of mean quantities. Despite the fact that the presumed β-PDF model is carried out by using reasonable computational efforts, the Monte Carlo PDF causes well capturing turbulence-chemistry interaction. Kyne et al. [16] used two combustion models including equilibrium model using PDF look up table approach to model three-dimensional turbulent combustion within air spray combustion. In addition, they compared the obtained results from k-ε and Reynolds stresses turbulent model. Guo et al. [17] proposed a presumed joint PDF model of turbulent combustion. They compared four combustion models: Arrhenius, eddy break-up (EBU), laminar flamelet, and PDF model. The results of both presumed PDF model and the laminar flamelet model agree well with the experiments. However, the obtained results from the other models did not have an acceptable accuracy. Cao et al. [18] applied a joint PDF method for a lifted turbulent jet flame with H_2/N_2 fuel. They showed this method can capture some flame parameters such as velocity, mixture fraction, and species concentration very well. Kim and Kim [19] experimentally investigated the length of an oxy-fuel flame. They proposed a correlation between dimensionless flame length and the fire Froude number. Khelil et al. [20] used numerical simulation to predict the pollutant emissions NO_x in a high swirling non-premixed confined flame using β-PDF model coupled with

Reynolds stress turbulence model. Kim et al. [21] studied a 0.2 MW oxy-fuel combustor experimentally for various range of oxidant velocity with measuring temperature and some species such as NO. Their results showed that the velocity is a significant parameter in NO level control.

In this study, a numerical solution is adopted for a non-premixed coaxial oxy-fuel turbulent flame using FLUENT commercial software [22]. Two-equation turbulence model is used. Two models of this type are used in the simulation and the results are compared in order to choose the appropriate model for an oxy-fuel turbulent flame. The presumed PDF model is employed to consider turbulence-combustion interactions. NO_x formation is also numerically predicted in the flame zone. The obtained results are compared with the experimental data of Ditaranto et al. [23].

2. Governing equations

Conservative equations for a steady state reacting flow are used here. A generalized equation includes overall mass, momentum, energy, and chemical species concentration equation can be written as [24]:

$$\frac{\partial}{\partial z}(\rho U\phi) + \frac{1}{r}\frac{\partial}{\partial r}(\rho V\phi) =$$
$$\frac{\partial}{\partial z}(\Gamma_\phi \frac{\partial \phi}{\partial z}) + \frac{1}{r}\frac{\partial}{\partial r}(r\Gamma_\phi \frac{\partial \phi}{\partial r}) + S_\phi \qquad (1)$$

Where quantity ϕ refers to the special equation. For $\phi=1$, a velocity component, h and Y_i it yields conservation equation of mass, momentum, energy, and species mass fraction, respectively. S_ϕ is the source term in the conservation equations.

3. Turbulence model

Because of complexity of flow due to turbulence, reaction process and interaction between them, choosing an appropriate turbulence model has a crucial effect on the simulation. Unfortunately, no single turbulence model is universally accepted for all types of flow [25]. In the current study, the simulation is performed with two-equation turbulence models:

3.1. Standard k-ε turbulence model

Ske [26] is a semi-empirical model which has been established upon two equations: an equation for the turbulence kinetic energy (k) and another equation for its dissipation rate (ε). Accuracy and economy for many types of turbulent flow allowed its frequent use as a widely used turbulence model. Modeling of dissipation rate (ε) is a weakness of the model. The spreading rate in planar jets is well predicted by this model, but prediction of the spreading rate for axisymmetric jets is amazingly poor, which is considered to be mainly due to the modeled dissipation equation. In addition, the dissipation rate equation of Ske model does not always give the suitable length scale for turbulence. The transport equations for the turbulence kinetic energy (k) and its dissipation rate (ε) are written as follows:

$$\frac{\partial}{\partial x_i}(\rho k u_i) = \frac{\partial}{\partial x_i}[(\mu + \frac{\mu_t}{\sigma_k})\frac{\partial k}{\partial x_i}]$$
$$+ G_k + G_b - \rho\varepsilon - Y_M \qquad (2)$$

$$\frac{\partial}{\partial x_i}(\rho \varepsilon u_i) = \frac{\partial}{\partial x_i}[(\mu + \frac{\mu_t}{\sigma_\varepsilon})\frac{\partial \varepsilon}{\partial x_i}]$$
$$+ C_{1\varepsilon}\frac{\varepsilon}{k}(G_k + C_{3\varepsilon}G_b) - C_{2\varepsilon}\rho\frac{\varepsilon^2}{k} \qquad (3)$$

Where, G_k and G_b denote the generation of turbulent kinetic energy because of the mean velocity gradients and buoyancy, respectively. Y_M also denotes the contribution of the fluctuating dilation in turbulence to the overall dissipation rate. $C_{1\varepsilon}$, C_μ, and $C_{3\varepsilon}$ are constants. σ_k and σ_ε are the turbulence Prandtl numbers for k and ε, respectively. The turbulent eddy viscosity is introduced as:

$$\mu_t = \rho C_\mu \frac{k^2}{\varepsilon} \qquad (4)$$

The constant values of the model are [26]:
$C_{1\varepsilon}$ = 1.44, C_μ = 0.09, $C_{2\varepsilon}$ = 1.92, σ_k = 1.0 and σ_ε = 1.3

3.2. Realizable k-ε turbulence model

Rke [27] is different from Ske model in two main features. Firstly, the turbulence eddy viscosity in this model is calculated by different formulation including the variable C_μ which is introduced as a function of local strain rate and rotation of the fluid. It is motivated to avoid unphysical values of the normal stresses because some of them may be negative in k-ε model. Secondly, this model utilizes different source and sink terms in the transport equations. For example, the ε transport equation does not involve the production of k in G_k term, while in the other k-ε models it does not. Additionally, the destruction term (second term in the right hand of Eq. 3) does not have a singularity point because its denominator does not become zero; even though k becomes zero or negative. Due to its prominent features of the model, Rke has been used in turbulent combustion in some previous studies [25, 28, 29]. However, the model has many advantages for flow simulation including strong streamline curvature, vortices, rotations, and the spreading rate of planner and round jets. As a limitation of the model, when the computational domain compounds both stationary and rotating fluid zones, the formulation of the model necessitates the non-physical turbulent viscosity. k transport equation is the same as in Ske model, while the ε equation in this model differs from that of Ske model and is written as follows:

$$\frac{\partial}{\partial x_i}(\rho \varepsilon u_i) = \frac{\partial}{\partial x_i}[(\mu + \frac{\mu_t}{\sigma_\varepsilon})\frac{\partial \varepsilon}{\partial x_i}]$$
$$- \rho C_2 \frac{\varepsilon^2}{k + \sqrt{v\varepsilon}} + C_{1\varepsilon}\frac{\varepsilon}{k}C_{3\varepsilon}G_b \tag{5}$$

In the Rke model, C_μ is not a constant and it is defined as:

$$C_\mu = \frac{1}{A_0 + A_s(kU^*/\varepsilon)} \tag{6}$$

Finally, the constants are:
$C_{1\varepsilon} = 1.44$, $C_2 = 1.9$, $\sigma_k = 1.0$ and $\sigma_\varepsilon = 1.2$
The other details containing the constants A_0 and A_s are presented in [27].

4. Turbulence-combustion interactions

Because of the fluctuating characteristics of the turbulent mixing process, the probability density function is a skilled method for the cases including combustion process and turbulent flow. In this study, the presumed PDF model with the assumption of its fast chemistry is employed. In this model, PDF is defined in terms of two parameters: the mean and its variance of scalar quantity. Due to better results for the turbulent reacting flow in comparison to the other PDF models, β-PDF model [9] is used to calculate the thermodynamic properties.

In the presumed β-PDF model, the mixture fraction, f, is defined in terms of mass fraction of specie i, Y_i:

$$f = \frac{Y_i - Y_{i,ox}}{Y_{i,f} - Y_{i,ox}} \tag{7}$$

where the subscripts f and ox denote the fuel, and oxidant streams, respectively.

The transport equations of mean mixture fraction, $\bar{f}$ and its variance, $\overline{f'^2}$, are:

$$\frac{\partial}{\partial t}(\rho \bar{f}) + \frac{\partial}{\partial x_i}(\rho u_j \bar{f}) = \frac{\partial}{\partial x_i}(\frac{\mu_t}{\sigma_t}\frac{\partial \bar{f}}{\partial x_i}) \tag{8}$$

$$\frac{\partial}{\partial t}(\rho \overline{f'^2}) + \frac{\partial}{\partial x_i}(\rho u_i \overline{f'^2}) = \frac{\partial}{\partial x_i}(\frac{\mu_t}{\sigma_t}\frac{\partial \overline{f'^2}}{\partial x_i})$$
$$+ C_g \mu_t(\frac{\partial \bar{f}}{\partial x_i}) - C_d \rho \frac{\varepsilon}{k}\overline{f'^2} \tag{9}$$

where the constants σ_t, C_g, and C_d are 0.85, 2.86, and 2.0, respectively. The relationship between the obtained time-averaged values from the above equations and the instantaneous mixture fraction is made by a PDF. This function is written as $p(f)$, which is the probability that the fluid exists in the state f. The method applies the mean values of species concentration and temperature. The mean species mass fraction and temperature, $\bar{\phi}_i$, is calculated from:

$$\bar{\phi}_i = \int_0^1 p(f)\phi_i(f)df \tag{10}$$

Where $p(f) = \frac{f^{\alpha-1}(1-f)^{\beta-1}}{\int f^{\alpha-1}(1-f)^{\beta-1}df}$

α and β are defined as follows:

$$\alpha = \bar{f}[\frac{\bar{f}(1-\bar{f})}{f'^2} - 1] \tag{11}$$

$$\beta = (1-\bar{f})[\frac{\bar{f}(1-\bar{f})}{f'^2} - 1] \tag{12}$$

For the non-adiabatic case, the mean enthalpy transport equation is described as:

$$\frac{\partial}{\partial t}(\rho \bar{h}) + \nabla.(\rho \vec{v}\bar{h}) = \nabla.(\frac{k_t}{c_p}\nabla \bar{h}) + S_h \tag{13}$$

where S_h is a source term because of radiation heat transfer to the wall boundaries. Chemical equilibrium is used for determining product mole fractions. According to the experiments [23], natural gas is used as the fuel.

5. Radiation heat transfer modeling

The radiation model may play a crucial role in the heat transfer to the surrounding walls in a combustor [30, 31]. The radiation heat transfer equation (RTE) for an absorbing, emitting, and scattering medium at position r and direction s is [32]:

$$\frac{dI(r,s)}{ds} = -(a + \sigma_s)I(r,s) + an^2\frac{\sigma T^4}{\pi}$$
$$+ \frac{\sigma_s}{4\pi} \times \int_0^{4\pi}I(r,s')\Phi(s,s')d\Omega' \tag{14}$$

Here r, s, s', a, n, σ_s, σ, I, T, Φ, and Ω' denote radial component vector, direction vector, scattering direction vector, absorption coefficient, refractive index, scattering coefficient, Stefan-Boltzmann constant ($= 5.672 \times 10^{-8}$ W.m^{-2}K^{-4}), total radiation intensity, local temperature, phase function, and solid angle, consecutively.

The discrete ordinate method (DOM) [33] is an appropriate model to simulate radiation heat transfer for the most applicable cases. It has been demonstrated that the model is a skillful and accurate method for PDF modeling of reacting flows [34]. Further information about this method can be found in [33].

6. Geometry and boundary conditions

Fig. 1 shows schematic geometry of the combustor taken from [23]. The inner diameter (2×R$_{fuel}$) and the outer diameter (2×R$_{oxy}$) of the coaxial flame are 7.5mm and 12.7mm, respectively. The combustor length, and radius, is 1m and 0.115m, respectively [23].

Fuel and oxidant axially enter the combustor with uniform velocities of 15.2 m.s^{-1} and 19.3 m.s^{-1},

respectively. The inlet turbulence kinetic energy and its dissipation rate are computed as [24]:

$$k = \frac{3}{2}(U_{ref}i)^2 \qquad \varepsilon = 0.16\frac{k^{1.5}}{\ell} \qquad (15)$$

In which i, ℓ, U_{ref} are defined as turbulence intensity, characteristic length, and inlet velocity, respectively. ℓ is predicted by [34]:

$$\ell = 0.07L \qquad (16)$$

The flow leaves the combustor with absolute pressure of 1bar. The standard wall function is applied to compute the tangential velocity near the wall. Temperature of the walls is fixed at a constant value of 1023K. For the radiation condition, the walls are assumed as a gray heat sink of emissivity 0.7.

Composition (mole fraction) details [23] of the reactants are presented in Table 1:

Table 1. Composition of fuel and oxidant [23]

Species	Mole fraction in fuel	Mole fraction in oxidant
CH_4	0.858	0
C_2H_6	0.093	0
C_3H_8	0.021	0
CO_2	0.009	0
N_2	0.02	0
O_2	-	1

7. Numerical procedure

The conservation equations for mass, momentum, energy, species as well as fuel combustion, kinetic energy turbulence and its dissipation rate are discretized using the finite volume method [24] and a second order upwind scheme. The SIMPLE algorithm is used to indicate the velocity and pressure coupling.

The criterion of convergence of the solution is that the maximum value of the normalized residual of energy equation and the other transport equations are chosen less than 10^{-6} and 10^{-4}, respectively. In order to prevent the divergence of the non-linear equations, appropriate under relaxation factors are employed. The grid is denser near the annular inlet zone due to the mixing and reaction processes. In the present study, it is found that the grid size of 24800 cells for the geometry ensures a grid independent solution (Table 2).

Table 2. Grid independency

Cells	Calculated outlet temperature (K)	Deviation from experimental results (1223K) [23]
12000	1453	19%
17500	1368	11%
24800	1301	6.4%
37000	1253	2.5%

8. NOx formation

NOx formation is an important topic in combustion because of its contribution to air pollution. *NO* is the most important species in the NOx emission for many type of flames [35]. NOx formation affects flow field negligibly; hence, it is post processed from the simulation. In addition, because of small rate formation of NOx by the kinetics mechanism, its concentration cannot be directly predicted by the PDF model.

To include NO formation for this type of flame, the thermal and prompt mechanisms are employed [36] and calculated by finite rate chemistry. For these two mechanisms, only the following NO species transport equation is required:

$$\frac{\partial}{\partial t}(\rho Y_{NO}) + \nabla.(\rho \vec{v} Y_{NO}) = \qquad (17)$$
$$\nabla.(\rho D \nabla Y_{NO}) + S_{NO}$$

in which, Y_{NO}, D, and S_{NO} are mass fraction, effective diffusion, and the source term, respectively.

S_{NO} can be calculated by the relation:

$$S_{NO} = M_{NO}(\frac{d[NO]}{dt}) \qquad (18)$$

Where M_{NO} is the molecular weight of NO and $\frac{d[NO]}{dt}$ is calculated by both thermal and prompt mechanisms.

The thermal NO formation rate is determined according to the highly temperature-dependent reactions referred as the extended Zeldovich mechanism [37]:

$$N_2 + O \Leftrightarrow NO + N \qquad (R1)$$

$$O_2 + N \Leftrightarrow NO + O \qquad (R2)$$

$$N + OH \Leftrightarrow NO + H \qquad (R3)$$

Assuming a quasi-steady-state for concentration of nitrogen atoms, the thermal NO formation rate becomes:

$$\frac{d[NO]}{dt} = 2\kappa_1[O][N_2]\frac{(1 - \frac{\kappa_{-1}\kappa_{-2}[NO]^2}{\kappa_1[N_2]\kappa_2[O_2]})}{(1 + \frac{\kappa_{-1}[NO]}{\kappa_2[O_2] + \kappa_3[OH]})} \qquad (19)$$

Where the reaction rates are: $\kappa_1 = 1.8 \times 10^8 \exp(-38370/T)$ $m^3 \cdot kmol^{-1}s^{-1}$, $\kappa_{-1} = 3.8 \times 10^7 \exp(-425/T)$, $\kappa_2 = 1.8 \times 10^4 T\exp(-4680/T)$ $m^3 \cdot kmol^{-1}s^{-1}$, $\kappa_{-2} = 3.81 \times 10^3 T\exp(-20820/T)$ $m^3 \cdot kmol^{-1}s^{-1}$, and $\kappa_3 = 7.1 \times 10^7 \exp(-450/T)$ $m^3 \cdot kmol^{-1}s^{-1}$ [37].

Taking partial equilibrium for concentration of O atoms [38]:

$$[O] = 36.64T^{0.5}[O_2]^{0.5}\exp(-27123/T) \qquad (20)$$

The prompt NO formation rate is depicted by the following equation [39]:

$$\frac{d[NO]}{dt} = f_c\kappa_{prompt}[O_2]^\alpha[N_2][fuel]\exp(\frac{E_a}{RT}) \qquad (21)$$

In which, α is the order of reaction and f_c is a correction factor which depends on the fuel type and fuel air ratio.

The value of κ_{prompt} and E_a are 6.4×10^6 and 72.5 Kcal.g^{-1} respectively.

Equations (19)-(21) are the instantaneous rates for a laminar flow field. Time averaged form of these equations is necessary to obtain the time mean value of the rates in the turbulent flames. In the present work, β-PDF of the normalized temperature, $f = (T - T_{min})/(T_{max} - T_{min})$, is employed for considering the effect of turbulent mixing on the *NO* formation.
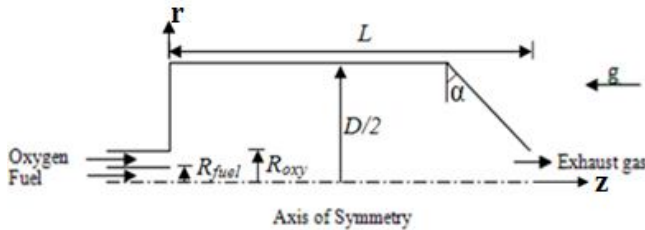

Fig. 1. Schematic geometry of the combustor

9. Results

In this part, two different k-ε turbulence models are examined to determine the characteristics of the coaxial oxy-fuel flame. It is obvious that the turbulence has an important effect on the flow field and consequently thermal characteristics of the flow, especially in a combustion process. Hence, choosing a suitable model for turbulence modeling plays an important role in the simulation. Compared with two-equation turbulence models, Ske model is the complete and simplest one. Good accuracy and economy for many turbulent flows are other advantages of this model in industrial flow and heat transfer simulations. Rke model is more recent in comparison to Ske model, which is also employed in the present work.

Fig. 2a shows the predicted contours of temperature in the combustor. A conventional shape is obtained for the flame. Because of the flame zone, temperature rises significantly in vicinity of the center of the combustor and decreases near the wall. In this view, the shape of the contours is slightly different for the two models.

Fig. 2b illustrates the streamlines in the combustor. Because of a sudden expansion in the geometry of the combustor, a recirculation zone is created. This zone increases the turbulent mixing and reduces the temperature of the flame zone and post flame zone due to diluting the reactants and thus, it can lead to reduction of *NO* concentration level [21]. Recirculation of the hot combustion products to the unburned inlet mixture also causes prevention of the lift-off of the flame and helps to stabilize it. As shown in this figure, Ske model predicts a longer recirculation zone (extended to about z = 680 mm) in comparison with that of the Rke model (which extend to about z = 640 mm). Entering more hot products in the unburned mixture by the recirculation zone flow may cause the combustion to take place faster.

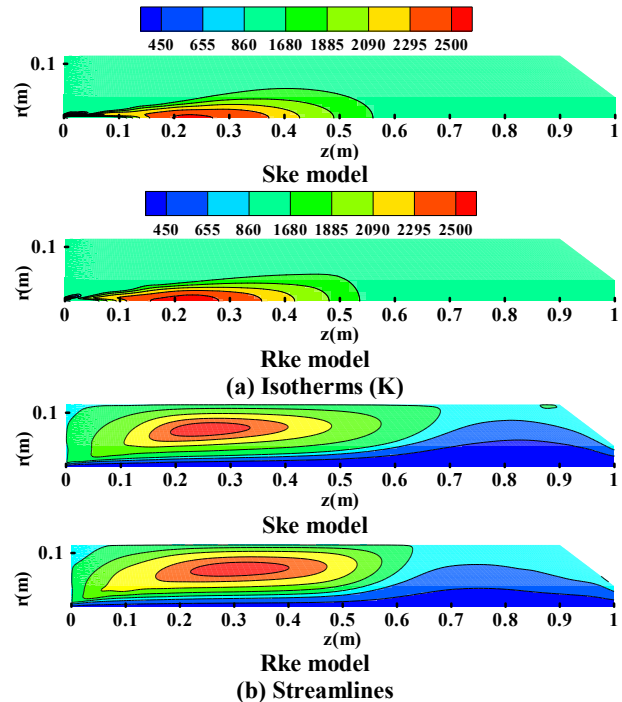**Fig. 2. a) Isotherms and b) Streamlines plots in the combustor with two turbulence models**

Experimental and numerical axial velocities are demonstrated in Figs 3(a-c). Fig. 3a shows the axial velocity (U) versus the radial distance at z = 40mm. The trend of predicted results for both models is similar to the experimental data. Both models over-estimate U at r<5mm, while at r>9mm, these models result in almost the same U values. The over-prediction for Ske model near the central region is mainly due to an overestimation of turbulence kinetic energy [40]. As can be seen in Fig. 3a, the predicted location of maximum U is slightly shifted to the centerline in comparison with the measured data of [23]. U at z = 100mm is shown in Fig. 3b. It is shown that Ske model over-estimates U at r<7.5mm and under-estimates U at r>7.5mm. Fig.3b shows that Ske model does not have an acceptable trend in comparison with the experimental data, while Rke model has a more reasonable behavior. At r<7mm, the results of Rke model approximately lie on the experimental data. In this figure, for radial distances greater than 10mm, Rke model has a better prediction with 12% relative error on average than Ske model with about 30% relative average error. Comparison of U in z = 40 mm and z = 100 mm (Figs 3a and 3b) shows that the maximum velocity decreased at z = 100 mm because of the mixing process, while its location shifted to the right.

Fig. 3c gives U at z = 170 mm. The trend of the obtained U with Rke model is almost the same compared with the experiment. The obtained U with Ske model approximately coincides at r<5mm, but it under-estimates at r>5mm with more deviation than Rke model from the experimental results. U profiles show that the magnitude of velocity in the combustor can approach to a value greater than the maximum inlet velocity due to the combustion phenomenon.

(a)

(b)

(c)
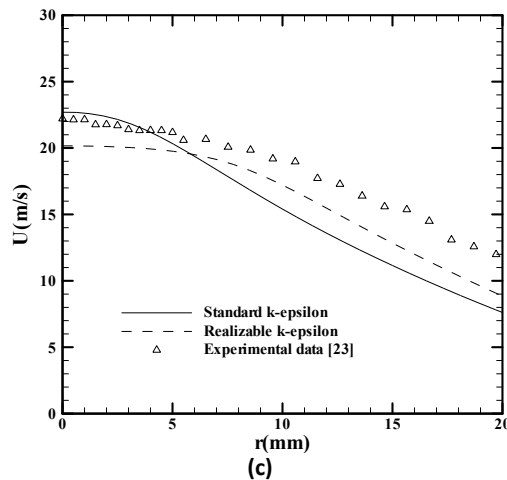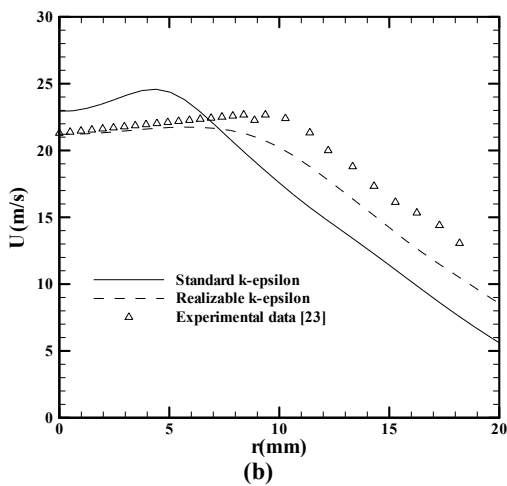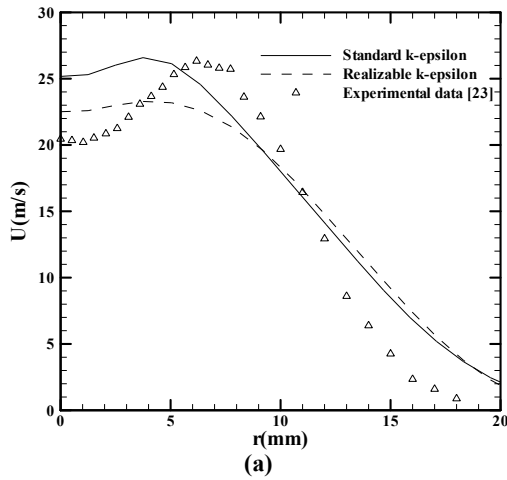
Fig. 3. Axial velocity profile at
a) z = 40mm b) z = 100mm and c) z = 170mm
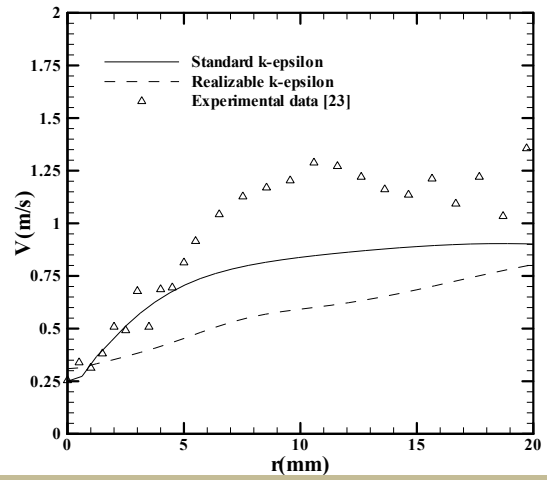
Fig. 4. Radial velocity at z = 170mm

Fig. 4 shows the radial velocity (V) at z = 170mm. The velocity is under-estimated by both models. However, Ske model gives better prediction of the velocity by approximately 20% error on average.

Fig. 5 illustrates the radial profile of *NO* pollutant concentration at z = 110 mm. In Rke model, the main part of the profile is over-estimated (r>8mm), but it has a very good trend with approximately 14% error on average. The *NO* concentration profile for Ske model is under-estimated as compared with the experimental data [23]. Ske turbulence model overestimates turbulence kinetic energy for most shear flows and since the combustion model determines reaction rates and heat release by using the turbulence data from the turbulence model, the peak temperatures are too low, which has a dramatic influence on the *NO* production rates [40-41]. However, this trend violently captures the shape of the experimental profile.
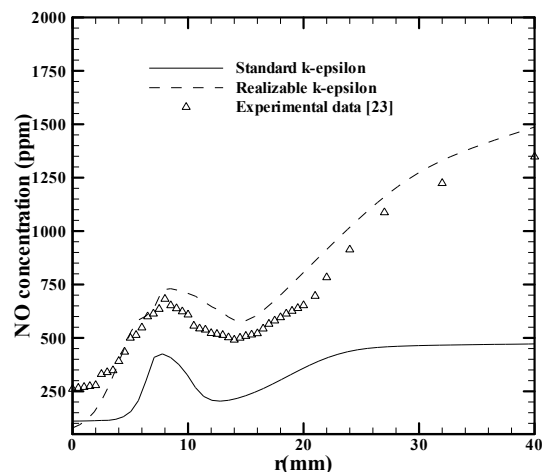
Fig. 5. NO concentration at z = 110 mm

Table 3. Exhaust gas temperature and flame length for various results	
	Exhaust gas temperature (K)
Ske model	1194.03
Rke model	1192.10
Experimental data [23]	1223.15

The temperature of the exhaust gas at combustor exit is compared with a mass-weighted average integral of temperature in Table 3. Both models predict the exhaust gas temperature properly; Ske and Rke models have 2.5% and 2.4% relative errors, respectively.

10. Conclusions

In this study, a coaxial oxy-fuel flame is simulated to predict turbulent flow behavior and temperature distribution using a presumed β-PDF model. The DO radiation heat transfer model was also employed. Numerical results from two turbulence models namely Ske and Rke were compared with the experimental data. The geometry of the combustor led to a recirculation zone, which can reduce temperature of the flame zone and NO level. It was found that Rke model provides better prediction of axial velocity and NO concentration profile than those in Ske model. The prediction of the axial velocity is more accurate in the vicinity of the centerline. Both models predict the temperature of the exhaust gas fairly well. Based on the results in the paper, numerical simulation with Rke accompanied by the PDF model is an appropriate tool to predict the flow and temperature behavior in a non-premixed oxy-fuel flame.

Acknowledgment

Nomenclature

a	absorption coefficient
c_p	specific heat capacity at constant pressure
$C_{1\varepsilon}$, C_2, $C_{3\varepsilon}$	turbulence model constants
C_g, C_d	PDF model constants
E_a	activation Energy
f	mixture fraction
f'^2	mixture fraction variance
G_k, G_b	generation of turbulent kinetic energy
g	gravitational acceleration
h	species enthalpy
I	total radiation intensity
k	turbulence kinetic energy
L	combustor length
ℓ	characteristic length
n	refractive index
NO_x	nitrogen oxides
M	molecular weight
$p(f)$	probability density function
S_φ, S_h	source terms
r, z	radial and axial coordinates
R	universal gas constant
s	direction vector
s'	scattering direction vector
T	temperature
U, V	axial and radial component of velocity
u_i	velocity components
x_i	coordinates representative
Y_i	mass fraction of species i

Greek symbols

α	order of reaction
Γ_φ	generalized effective transport coefficient
ε	dissipation rate of turbulence kinetic energy
κ	reaction rate constant
μ	dynamic viscosity
μ_t	turbulent eddy viscosity
σ	Stefan–Boltzmann constant
σ_k, σ_ε	turbulence model constants
σ_s	scattering coefficient
σ_t	PDF model constants
υ	kinematic viscosity
ρ	density
Φ	phase function
φ	generalized variable
Ω'	solid angle

subscripts

f	fuel
ox	oxidant

Abbreviation

DOM	discrete ordinate model
Ske	standard k-epsilon turbulence model
Rke	realizable k-epsilon turbulence model

References

[1]   Jones, W. P., Launder, B. E., "*The calculations of low-Reynolds number phenomena with a two-equation model of turbulence*", International Journal of Heat and Mass Transfer, vol.16, pp. 1119- 1130, 1973.

[2]   Chien, K. Y., "*Predictions of channel and boundary layer flow with a low-Reynolds-number turbulence model*", AIAA Journal, vol. 20, pp. 33-38, 1982.

[3]   Yang, Z., Shih, T. H., "A new time scale based k-ε model for near wall turbulence", AIAA Journal, vol. 31, pp. 1191-1198, 1993.

[4]   Shih, T. H., Lumley, J. L., "*Kolmogorov behavior of near wall turbulence and its application in turbulence modeling*", NASA TM 105663.

[5]   Bardina, J., Ferziger, J. H., Reynolds, W. C., "*Improved turbulence models based on large eddy simulation of homogeneous, incompressible*", turbulent flows. Rept. No. TF-19, Stanford University, Stanford, CA, 1983.

[6] Nisbet, J., Davidson, L., Olsson, E., "*Analysis of two fast-chemistry combustion models and turbulence modeling in variable density flow*", computational fluid dynamics, vol. 1, pp. 557-563, 1992.

[7] Ellzey, J.L., Laskey, K.J., Oran, E.S., "*A study of confined diffusion flames*", Combustion and. Flame, vol. 84, pp. 249-264, 1991.

[8] Poinsot, T., Veynante, D., "*Theoretical and numerical combustion*", Philadelphia, PA: R.T. Edwards, Inc., 2001.

[9] J. Hannon, S. Hearn, L. Marshall and W. Zhou, "Assessment of CFD approaches to predicting fast chemical reactions", in: Annual AICH meeting, chemical and biological reactors session, Miami Beach, FL, November 15-20, 1998.

[10] Hartick, J.W., Tacke, M., Früchtel, G., Hassel, E.P., Janicka, J., "Interaction of turbulence and radiation in confined diffusion flames", Symposium of Combustion, vol. 26, pp. 75-82, 1996.

[11] Sautet, J. C., Ditaranto, M., Samaniego, J. M., Charon, O., "*Properties of turbulence in natural gas-oxygen diffusion flames*", International Communication in Heat and Mass Transfer, vol. 26, pp. 647-656, 1999.

[12] Aroussi, A., Pickering, S.J., Tarr, S., "*Momentum interchange in a burner bank*", Journal of Fuel, vol. 79, pp. 1439-1448, 2000.

[13] Liakos, H. H., Founti, M. A., Markatos, N. C., "*Modelling of stretched natural gas diffusion flames*", Applied Mathematical Modeling, vol. 24, pp. 419-435, 2000.

[14] Demoulin, FX., Borghi, RA., "*Assumed PDF modeling of turbulent combustion*", Combustion Science and. Technology, vol. 158, pp. 249-271, 2000.

[15] Repp, S., Sadiki, A., Schneider, C., Hinz, A., Landenfeld, T., Janicka, J., "*Prediction of swirling confined diffusion flame with a Monte Carlo and a presumed PDF model*", International Journal of Heat and Mass Transfer, vol. 45, pp. 1271-1285, 2002.

[16] Kyne, A. M., Pourkashanian, M., Wilson, CW., Williams, A., "*Validation of a flamelet approach to modeling 3-D turbulent combustion within an airspray combustor*", ASME paper, No. GT-2002-30096, 2000.

[17] Guo, Z. M., Zhang, HQ., Chan CK., Lin, W. Y., "*Presumed joint probability density function model for turbulent combustion*", Journal of Fuel., vol. 82, pp. 1091-1101, 2003.

[18] Cao, R. R., Pope S.B., Masri, A.R., "*Turbulent lifted flames in a vitiated co-flow investigated using joint PDF calculations*", Combustion and Flame, vol. 142, pp. 438-453, 2005.

[19] Kim, H.K., Kim, Y., "*Studies on combustion characteristics and flame length of turbulent oxy−fuel flames*", Journal of Energy and Fuel, vol. 21, pp. 1459-1467, 2007.

[20] Khelil, A., Naji, H., Loukarfi, L., Mompean, G., "*Prediction of a high swirled natural gas diffusion flame using a PDF model*", Journal of Fuel, vol. 88, p.p. 374-381, 2009.

[21] Kim, H.K., Kim, Y., Lee S.M., Ahn, K.Y., "*Emission characteristics of the 0.2 MW oxy-fuel combustor*", Journal of Energy and Fuel, vol. 23, pp. 5331-5337, 2009.

[22] FLUENT User's Manual, Version 6.3.26, 2006.

[23] Ditaranto, M., Sautet, J. C., Samaniego, J. M. "*Structure aspects of coaxial oxy-fuel flames*", Experiments in Fluids., vol. 30, pp. 253-261, 2001.

[24] Versteeg H. K., Malalasekera, W., "*An introduction to computational fluid dynamics: the finite volume method*", Addison Wesley-Longman, 1995.

[25] Veynante, D., Vervisch, L., "*Turbulent combustion modeling*", Progress in Energy and. Combustion Science, vol. 28, No. 3, pp. 193-266, 2002.

[26] Launder, B. E., Spalding, D. B., "*Lectures in mathematical models of turbulence*", Academic Press, London, England, 1972.

[27] Shih, T. H., Lion, WW., Shabbir, A., Yang, Z., Zhu, J., "*A new k–ε eddy-viscosity model for high Reynolds numerical turbulent flows-model development and validation*", Journal of Computational Fluids, vol. 24, pp. 227-238, 1995.

[28] Zhou, L.X., Qiao, X.L., "*A USM turbulence-chemistry model for simulating NOx formation in turbulent combustion*", Journal of Fuels, vol. 81, No. 13, pp. 1703-1709, 2002.

[29] Zhou, L.X., Wang, F., Zhang, J., "*Simulation of swirling combustion and NO formation using a USM turbulence-chemistry model*", Journal of Fuels, vol. 82, No. 13, pp. 1579-1586, 2003.

[30] Chen, J. Y., Chang, W. C., "*Flamelet and PDF modeling of CO and NOx emissions from a turbulent, methane hydrogen jet nonpremixed flame*", Symposium (International) on Combustion, vol. 26, No. 2, p.p. 2207-2214, 1996.

[31] Naik, S. V., Laurendeau, N. M., Cooke, J. A., Smooke, M. D., "*Quantitative laser-saturated fluorescence measurements of nitric oxide in counter-flow diffusion flames under sooting oxy-fuel conditions*", Combustion and Flames, vol. 134, p.p. 425-431, 2003.

[32] M. F. Modest, "Radiative heat transfer", Academic Press, 2003.

[33] Fiveland, W. A., "*Discrete-ordinate solution of radiative transport equation for rectangular enclosure*", Journal of Heat and Mass Transfer, vol. 40, pp. 699–706, 1984.

[34] Bazdidi-Tehrani, F., Zeinivand, H., "*Presumed PDF modeling of reactive two-phase flow in a three dimensional jet-stabilized model combustor*", Journal of Energy Conversion and Management, vol. 51 pp. 225-234, 2010.

[35] Drake, M.C., Correa, S.M., Pitz, R.W., Shyy, W., Fenimore, C.P., "*Superequilibrium and thermal nitric oxide formation in turbulent diffusion flames*", Combustion and Flames, vol. 69, No. 3, pp. 347-365, 1987.

[36] Bin, J., Hongying, L., Guoqiang, H., Xingang, L., "*Study on NOx Formation in CH4/Air Jet Combustion*", Chinese Journal of Chemical Engineering, vol. 14, No. 6, p.p. 723-728, 2006.

[37]   Turns, S. R., "*An introduction to combustion: Concept and applications*", McGraw Hill, 2000.

[38]   Raine, R.R., Stone, C.R., Gould, J., "*Modeling of nitric oxide formation in spark ignition engines with a multizone burned gas*", Combustion and Flames, vol. 102, No. 3, pp. 241-255, 1995.

[39]   De Soete, G., "*Overall reaction rates of NO and N_2 formation from fuel nitrogen*", Processing Combustion Institute, pp. 1093-1102, 1974.

[40]   Kurreck, M., Willmann, M., Wittig, S., "*Prediction of the three-dimensional reacting two-phase flow within a jet-stabilized combustor*", Engineering of Gas Turbine Power Journal, vol. 120, p.p.77-83, 1998.

[41]   Yilmaz, B., Ozdogan, S., Gokalp, I., "*Numerical study on flame-front characteristics of conical turbulent lean premixed methane/air flames*", Journal of Energy and Fuel, vol. 23, p.p. 1843-1848, 2009.